

Numerical Simulation of Combustion Chamber Without Cavity at Mach 3.12

K.M. Pandey, A.P. Singh

Abstract— *In this Simulation, supersonic combustion of hydrogen at Mach 3.12 has been presented. The combustor has a single fuel injection perpendicular to the main flow from the base. Finite rate chemistry model with K-ε model have been used for modeling of supersonic combustion. The pressure rise due to the combustion is not very high on account of global equivalence ratio being quite low. Within the inlet the shock-wave-boundary- layer interactions play a significant role. The combustor without cavity is found to enhance mixing and combustion while increasing the pressure loss, compared with the case without cavity to the experimental results. The OH mass fraction is less almost by an order to that of water mass fraction. The OH mass fraction decreases as the gas expands around the injected jet and the local mixture temperature falls, However OH species are primarily produced in the hot separation region upstream of the jet exit and behind the bow shock and convected downstream with shear layer. The geometry results shows the better mixing in combustion chamber, caused by more extreme shear layers and stronger shocks are induced which leads loss in total pressure of the supersonic stream.*

Keywords— *Hydrogen, Shear layers, Stabilization, stagnation temperature, Supersonic combustion.*

I. INTRODUCTION

An invention attributed to Rene Lorin of France in 1913, the ramjet is a remarkable air-breathing engine in its conceptual simplicity. Lacking moving parts and achieving air compression only through internal geometry change, it is capable of extending the operation beyond flight speed when the gas-turbine engine becomes inefficient. The ramjet does not, however, operate from takeoff, and its performance is low at subsonic speeds because the air dynamic pressure is not sufficient to raise the cycle pressure to the efficient operational values. Above a flight speed of around Mach

3, cycles using rotating machinery, i.e., compressors, are no longer needed to increase the pressure, which can now be achieved by changes in area within the inlet and the diffuser leading to the combustion chamber. Engines without core rotating machinery can operate with a higher maximum cycle temperature as the limit imposed by the turbine presence on the cycle maximum temperature can now be increased. The ramjet cycle with subsonic air speed at the combustion chamber entrance becomes more efficient. As the speed further increases, the terminal shock associated

with subsonic combustion leads to both significant pressure losses and elevated temperatures that preclude, in great part, recombination-reaction completion, thereby resulting in considerable energy loss. It becomes more efficient to maintain the flow at supersonic speed throughout the engine and to add heat through combustion at supersonic speed. The subsonic conditions in the combustion chamber in the former require the presence of a physical throat in the nozzle to maintain the desired inlet operational conditions, whereas the supersonic combustion chamber, in fact, requires an area increase as heat is released through combustion.

A general review is presented by Zabaykin and Smogolev[1] of the worldwide evolution of ramjet propulsion since the Wright brothers first turned man's imagination to fly into a practical reality. Ramjet and scramjet propulsion technology has matured dramatically over the years in support of both military and space access applications, yet many opportunities remain to challenge future generations of explorers. Ingenito and Bruno [2] studied on physics of supersonic combustion towards the scramjet powered vehicles. Despite studies on supersonic combustion dating back to the 1950s, there are still numerous uncertainties and misunderstandings on this topic. The following questions need to be answered: How does compressibility affect mixing, flame anchoring, and combustion efficiency? How long must a combustor be to ensure complete mixing and combustion while avoiding prohibitive performance losses? How can reacting turbulent and compressible flows be modeled? Tien, and Stalker [3] investigated the process involved in chemical energy release by combustion in a supersonic, constant pressure, hydrogen-air laminar mixing layer was studied computationally, with a chemical kinetics model involving nineteen reactions and eight species. To try to find out the physical reason for the different trends of the pressure curves observed in an experimental supersonic combustor at two different initial air stream temperatures. Two initial air stream temperatures corresponding to the two experimental cases are chosen such that the higher temperature yielded a shorter ignition distance, and the lower temperature yielded a longer ignition distance.

Ben-Yakar et al. [4] describes ongoing research efforts in the scramjet community on cavity flame holders, a concept for flame holding and stabilization in supersonic combustors. However, comprehensive studies are needed to determine the optimal configuration that will yield the most effective flame holding capability with minimum losses.

Manuscript Received Dec.26, 2011.

K.M. Pandey, Professor and Dean (FW) Department of Mechanical Engineering, NIT Silchar Assam. (E-mail: kmpandey2001@yahoo.com).

A.P. Singh, Lecturer Department of Mechanical Engineering, NIT Silchar Assam. (E-mail: hello2apsingh@gmail.com).

The flow field characteristics of cavities and research efforts related to cavities employed in low and high-speed flows are summarized. Open questions impacting the effectiveness of the cavities as flame holders in supersonic combustors are discussed.

A comprehensive DES quality numerical analysis has been carried out by Choi et al. [5] for reacting flows in constant-area and divergent scramjet combustor configurations with and without a cavity. Transverse injection of hydrogen is considered over a broad range of injection pressure. The corresponding equivalence ratio of the overall fuel/air mixture ranges from 0.167 to 0.50. The work features detailed resolution of the flow and flame dynamics in the combustor, which was not typically available in most of the previous studies. In particular, the oscillatory flow characteristics are captured at a scale sufficient to identify the underlying physical mechanisms. Much of the flow unsteadiness is related not only to the cavity, but also to the intrinsic unsteadiness in the flow field. The interactions between the unsteady flow and flame evolution may cause a large excursion of flow oscillation. The roles of the cavity, injection pressure, and heat release in determining the flow dynamics are examined systematically.

Experimental investigations were carried out by Anavaradham et al. [6] to study the acoustic radiation from a rectangular wall mounted cavity in a confined supersonic flow. The free-stream Mach number was maintained at 1.5 and the cavity length-to-depth ratio was varied from 0.43 to 5.0. Acoustic measurements made on the top wall show jumps in the dominant frequency as the cavity behavior changes from shallow to-square-to-deep cavity. The numerical study also predicts the frequency jump observed in experiments.

Ben-Yakar et al. [7] describes an experimental effort to characterize the flame-holding process of a hydrogen jet injected into a high total enthalpy supersonic cross flow. An expansion tube is used to provide a correct simulation of true flight combustion chemistry, including ignition delay and reaction times. This indicates that combustion of hydrogen and air in these high total enthalpy conditions is a mixing limited process. It is evident from the results that improved injection schemes will be required for practical applications in scramjet engines.

The characteristics of supersonic cold flows over cavities were investigated by Fang et al. [8] experimentally and numerically, and the effects of cavities of different sizes on supersonic flow field were analyzed. The results indicate that the ratio of length to depth L/D within the range of 5–9 has little relevance to integral structures of cavity flow. The bevel angle of the rear wall does not alter the overall structure of the cavity flow within the range of 30° – 60° , but it can exert obvious effect on the evolution of shear layer and vortexes in cavities.

Jeung et al. [9] renewed interest on the scramjet engine has been demonstrated through the many international activities along the several Asia-Pacific countries. Here, a short review of current activities on supersonic combustion in a scramjet engine will be addressed followed by the discussions on the review of numerical simulation on supersonic combustion phenomena related with scramjet engine combustors and ram accelerator. Emphasis was put

on the grid refinement, scheme, unsteadiness and phenomenological differences.

Kim et al. [10] studied the numerical investigations concerning the combustion enhancement when a cavity is used for the hydrogen fuel injection through a transverse slot nozzle into a supersonic hot air stream. The cavity is of interest because recirculation flow in cavity would provide a stable flame holding while enhancing the rate of mixing or combustion. Several inclined cavities with various aft wall angle, offset ratio and length are evaluated for reactive flow characteristics. The cavity effect is discussed from a viewpoint of total pressure loss and combustion efficiency. The combustor with cavity is found to enhance mixing and combustion while increasing the pressure loss, compared with the case without cavity. But it is noted that there exists an appropriate length of cavity regarding the combustion efficiency and total pressure loss.

Recent results from combustion experiments reviewed in a direct-connect supersonic combustor are presented by Mathur et al. [11]. Successful ignition and sustained combustion of gaseous ethylene have been achieved using an injector/flameholder concept with low-angle, flush-wall fuel injection upstream of a wall cavity. Two interchangeable facility nozzles (Mach 1.8 and 2.2) were used to obtain combustor inlet flow properties that simulate flight conditions between Mach 4 and 6 at a dynamic pressure of 47.9 kPa. Mainstream combustion was achieved at equivalence ratios between 0.25 and 0.75 using only a spark plug and no other external ignition aids. Delta-force levels between 667 and 1779 N were measured, with corresponding combustor pressure ratios between 3.1 and 4.0. Video records of the flame zone show an intensely active combustion zone with rapid flame spreading. One-dimensional performance analysis of the test data indicates combustion efficiency around 80% with an average combustor skin friction coefficient of 0.0028

Activities in the area of scramjet fuel-air mixing and combustion associated with the Research and Technology Organization Working Group on Technologies for Propelled Hypersonic Flight are described by Drummond et al. [12]. Work discussed in this paper has centered on the design of two basic experiments for studying the mixing and combustion of fuel and air in a scramjet. Simulations were conducted to aid in the design of these experiments. The experimental models were then constructed, and data were collected in the laboratory. Comparison of the data from a coaxial jet mixing experiment and a supersonic combustor experiment with a combustor code were then made and described. This work was conducted by NATO to validate combustion codes currently employed in scramjet design and to aid in the development of improved turbulence and combustion models employed by the codes.

Hydrogen injection has been investigated numerically by Burtshell et al. [13] in a flow configuration caused by strong shock-boundary layer interaction named Viscous Mach Interaction (VMI). The geometry that leads to this configuration is used as a hypersonic inlet. The subsonic zone, because of boundary layer detachment, allows hydrogen to be injected along the wall of the central body where combustion

processes occur along a slip line when hydrogen is mixed with the incoming air flow far from the wall of the central body. High-resolution two-dimensional numerical simulations have been initiated by Haworth et al. [14] for premixed turbulent propane-air flames propagating into regions of non-homogeneous reactant stoichiometry. Simulations include complex chemical kinetics, realistic molecular transport, and fully resolved hydrodynamics (no turbulence model). Material and methods mathematical model

A. Governing Equations

The governing equations for a general coordinate comprise the mass conservation equation, the full Navier-Stokes equation, energy and species transport equations for a chemically reacting gas composed of N species as follows

$$\frac{\partial \bar{Q}}{\partial t} + \frac{\partial (\bar{F} - \bar{F}_v)}{\partial \xi} + \frac{\partial (\bar{G} - \bar{G}_v)}{\partial \eta} = \bar{S}$$

Where the conservative vector is \bar{Q} and the convection and viscous terms in the ξ and η direction are \bar{F} , \bar{G} and \bar{F}_v , \bar{G}_v respectively and defined as below. The source term for chemical reaction is \bar{S} .

$$\bar{Q} = \frac{1}{J} \bar{Q} = \frac{1}{J} \begin{pmatrix} \rho \\ \rho u \\ \rho v \\ \rho e_t \\ \rho Y_i \end{pmatrix}, \quad \bar{S} = \frac{1}{J} \bar{S} = \frac{1}{J} \begin{pmatrix} 0 \\ 0 \\ 0 \\ 0 \\ \dot{\omega}_i \end{pmatrix}$$

$$\bar{F} = \frac{1}{J} (\xi_x F + \eta_x G) = \frac{1}{J} \begin{pmatrix} \rho u \\ \rho u^2 + \xi_x P \\ \rho v u + \xi_y P \\ h \rho u \\ Y_i \rho u \end{pmatrix},$$

$$\bar{G} = \frac{1}{J} (\xi_y F + \eta_y G) = \frac{1}{J} \begin{pmatrix} \rho v \\ \rho u v + \eta_x P \\ \rho v^2 + \eta_y P \\ h \rho v \\ Y_i \rho v \end{pmatrix},$$

$$\bar{F}_v = \frac{1}{J} (\xi_x F_v + \eta_x G_v), \quad \bar{G}_v = \frac{1}{J} (\xi_y F_v + \eta_y G_v)$$

$$F_v = \begin{pmatrix} 0 \\ \tau_{xx} \\ \tau_{xy} \\ u\tau_{xx} + v\tau_{xy} - q_x \\ \rho D_i \frac{\partial Y_i}{\partial x} \end{pmatrix}, \quad G_v = \begin{pmatrix} 0 \\ \tau_{xy} \\ \tau_{yy} \\ u\tau_{xy} + v\tau_{yy} - q_y \\ \rho D_i \frac{\partial Y_i}{\partial y} \end{pmatrix}$$

The shear stress and heat flux in viscous terms may be

denoted by the following equations

$$\tau_{xx} = \frac{\mu}{Re_\infty} \left(\frac{4}{3} \frac{\partial u}{\partial x} - \frac{2}{3} \frac{\partial v}{\partial y} \right)$$

$$\tau_{yy} = \frac{\mu}{Re_\infty} \left(\frac{4}{3} \frac{\partial v}{\partial y} - \frac{2}{3} \frac{\partial u}{\partial x} \right), \quad \tau_{xy} = \frac{\mu}{Re_\infty} \left(\frac{\partial u}{\partial x} + \frac{\partial v}{\partial y} \right)$$

$$q_x = -\frac{1}{Re_\infty Pr (\gamma - 1)} K \frac{\partial T}{\partial x} - \frac{1}{Re_\infty Sc_\infty} \rho \sum_{i=1}^{N_s-1} h_i D_i \frac{\partial Y_i}{\partial x}$$

$$q_y = -\frac{1}{Re_\infty Pr (\gamma - 1)} K \frac{\partial T}{\partial y} - \frac{1}{Re_\infty Sc_\infty} \rho \sum_{i=1}^{N_s-1} h_i D_i \frac{\partial Y_i}{\partial y}$$

Where u and v are the velocity components in the x and y directions. Symbols Re_∞ , Pr, K, γ , and Sc_∞ are the Reynolds number, Prandtl number, thermal conductivity, specific heat ratio, and Schmidt number, respectively. D_i , h_i , and Y_i are diffusion coefficient, enthalpy and mass fraction for species i.

The transport properties are used in this study consists of viscosity, thermal conductivity, and diffusion coefficients, which can be represented by the sum of laminar (molecular) and turbulent components as follows:

$$\mu = \mu_l + \mu_t, \quad K = K_l + K_t, \quad D_i = D_{il} + D_{it}$$

B. K-ε Turbulence model

Modified k-ε model called Renormalization Group (RNG) is proposed by Yakhot et al. [22], which systematically removes all the small scale of turbulence motion from the governing equation by expressing their effect in terms of large scales and a modified viscosity.

$$\frac{\partial (\rho \kappa)}{\partial t} + \nabla \cdot (\rho \kappa u) = \text{div} [a_k \mu_{eff} \text{grad} \kappa] + H_k$$

$$\frac{\partial (\rho \varepsilon)}{\partial t} + \text{div} (\rho \varepsilon U) = \text{div} [a_k \mu_{eff} \text{grad} \kappa] + H_\varepsilon$$

Here the turbulence source term are defined as

$$H_k = 2\mu_t E_{ij} - \rho \varepsilon$$

and

$$H_\varepsilon = C_{1\varepsilon}^* \frac{\varepsilon}{\kappa} 2\mu_t E_{ij} \cdot E_{ij} - C_{2\varepsilon} \rho \frac{\varepsilon^2}{\kappa}$$

Turbulence viscosity is defined as

$$\mu_t = \rho C_\mu \frac{\kappa^2}{\varepsilon}$$

Closure coefficient are evaluated as

$$C_\mu = 0.0845, \quad \alpha_\kappa = \alpha_\varepsilon = 1.39, \quad C_{1\varepsilon} = 1.42$$

$$C_{2\varepsilon} = 1.68$$

$$\eta = \sqrt{\left(2E_{ij} \cdot E_{ij} \right)^{\frac{\kappa}{\varepsilon}}}$$

and

$$C_{1\varepsilon}^* = C_{1\varepsilon} - \frac{\eta(1-\eta/\eta_0)}{1+\beta\eta^3}$$

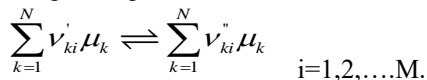
$$\eta_0 = 4.377$$

$$\beta = 0.012$$

Value of constant β is adjustable which is found from near the wall turbulence data.

C. Chemical Reaction Model

The present finite rate chemistry model includes seven species (H₂, O₂, N₂, H, O, OH, H₂O) and eight elementary reaction steps. Consider a chemical system of N species reacting through M reaction denoted as [133]:



Where μ_k is a symbol for species k. v'_{ki} and v''_{ki} are the stoichiometric coefficients of species k for i reactions. The reaction term is defined as:

$$\dot{\omega}_k = W_k \sum_{i=1}^M v_{ki} \hat{Q}_i$$

Where

$$\hat{Q}_i = \underbrace{K_{fi} \prod_{k=1}^N \left(\frac{\rho Y_k}{W_k} \right)^{v'_{ki}}}_{\text{forward-reaction}} - \underbrace{K_{ri} \prod_{k=1}^N \left(\frac{\rho Y_k}{W_k} \right)^{v''_{ki}}}_{\text{reverse-reaction}}$$

Using the empirical Arrhenius law,

$$K_{fi} = A_{fi} T^{\beta_i} \exp\left(-\frac{E_i}{RT}\right) = A_{ij} T^{\beta_i} \exp\left(-\frac{E_{ai}}{RT}\right)$$

Therefore, the source term is:

$$\dot{\omega}_k = W_k \sum_{i=1}^M v_{kj} \left[K_{fi} \prod_{k=1}^N \left(\frac{S_k}{W_k} \right)^{v'_{ki}} \right] - W_k \sum_{i=1}^M v_{ki} \left[K_{ri} \prod_{k=1}^N \left(\frac{S_k}{W_k} \right)^{v''_{ki}} \right]$$

The backward rates K_{ri} are computed through the equilibrium constants:

$$K_{ri} = \frac{K_{fi}}{\left(\frac{p_a}{RT} \right)^{\sum_{k=1}^N \exp\left(\frac{\Delta S_i^0 - \Delta H_i^0}{RT}\right)}}$$

Where ΔS_j^0 and ΔH_j^0 are entropy and enthalpy, respectively.

$$\dot{\omega}_k^{t+1} = W_k \sum_{i=1}^M v_{ki} \left[K_{fi,cv}^{t+1} \prod_{k=1}^N \left(\frac{S_{k,cv}^{t+1} + S_{k,cv}^{t+1}}{2W_k} \right)^{v'_{ki}} \right] - W_k \sum_{i=1}^M v_{ki} \left[K_{ri,cv}^{t+1} \prod_{k=1}^N \left(\frac{S_{k,cv}^{t+1} + S_{k,cv}^{t+1}}{2W_k} \right)^{v''_{ki}} \right]$$

II. RESULT AND DISCUSSION

Figure 1 shows the experimental work of Ben-yaker [14], an example of schlieren image for hydrogen injection case. While the unsteady features (coherent structures) are averaged to zero, some of the weak shocks such as upstream separation shock wave and downstream recompression wave are emphasized.

Figure 2 represents the contour of Mach number near the hydrogen injection point in which a separation shock, bow shock, Mach disk, barrel shock, barrel shock, UOI

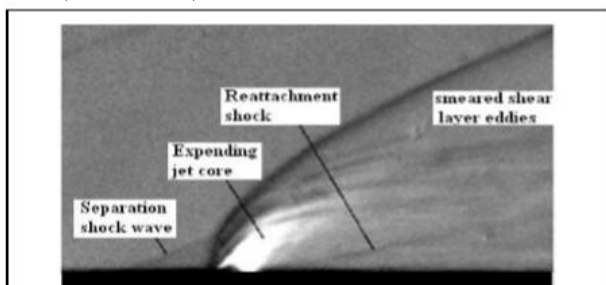


Figure 1 An example of schlieren image for hydrogen injection case.

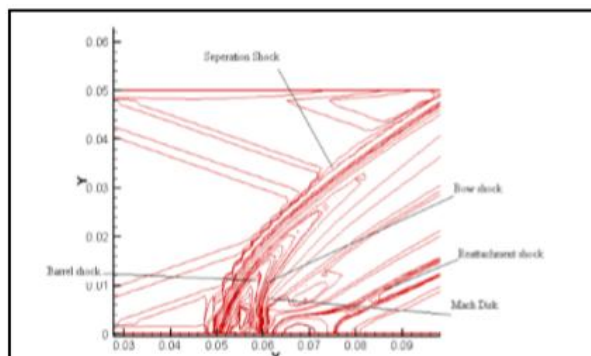


Figure 2 Contour of Mach number near injector

TABLE-1

Inflow Conditions Of The Air And The Hydrogen Jet.

| | Air | Hydrogen |
|------------------------|-------|-----------------|
| Ma | 3.12 | 1.5 |
| V[m/s] | 1182 | 2077 |
| P[10 ⁵ Pa] | .8 | .8 |
| P[kg/m ³] | 1.002 | 0.097 |
| yO ₂ | 0.232 | 0 |
| yN ₂ | 0.736 | 0 |
| yH ₂ O | 0.032 | 0 |
| yH ₂ | 0 | 1 |
| K[$\frac{m^2}{s^2}$] | 10 | 2400 |
| E[$\frac{m^2}{s^2}$] | 650 | 10 ⁸ |

shock and reattachment shock at downstream of the injector can be easily identified.

For the basic comparison with other results, the reactive flow field without cavity is solved with hydrogen injected perpendicular to the supersonic free stream. Figure 5 shows the contours of Mach number at 3.12, the deflection of path lines clearly shows the oblique shock wave from the upstream face of injection. Near the injector the flow is subsonic in separated region as it can be clearly visualized in contour of Mach number. While in the recalculated zone the Mach number is around 2.27. The small instantaneous fluctuations of the bow shock are observed to average into a smoother and slightly thicker one. The Mach number field shows that the flow is supersonic except for some transonic spot localized within the fuel-rich zone. Figure 6, Static pressure for the reacting flow on the lower and upper wall is quite different. The pressure rise due to the combustion is not very high on account of global equivalence ratio being quite low. Within the inlet the shock-wave-boundary-layer interactions play a significant role. When sufficiently strong, these shock waves impinge on the boundary layers that are sensitized by adverse pressure gradients caused by a pressure raise in the combustion chamber, leading to flow separations and producing several adverse effects on the inlet operation. Furthermore, the local boundary-layer distortion generates a new structure of shock waves and modifies the inlet-flow structure. Flame holding requires achieving a balance between the flame propagation speed and the fluid velocity. Because the fluid velocity exceeds the flame speed in supersonic combustion applications, the flame holding issue is solved by the generation of some sort of recirculation region that ensures sufficient residence time so that the processes involved - fuel-air mixing, ignition and chemical-reaction propagation - can take place to completion. Contours pressure shows the expansion fan around leading edge of injection. There is a recompression shock just near the injection point due to shear layer growth. Contour of static temperature shows the combustion and heat releases to be taking place and the flame spreads upwards as it moves along the wall. Contour of static temperature shows the combustion and heat release to be taking place in the upstream separation region under the adiabatic wall condition because no heat produced by the exothermic reaction is lost through the wall and temperature becomes more than 2700 K. The vicinity of the wall near the small recirculation as well as the downstream region of the injector is filled with unburned fuel gases injected through the injector. The temperature in that region is lower than the injected gas temperature because of under-expansion effects of the injected gas. The high temperature region is located near the upstream boundary of the jet above the small-scale re-circulation rather than at the center region of the small-scale recirculation.

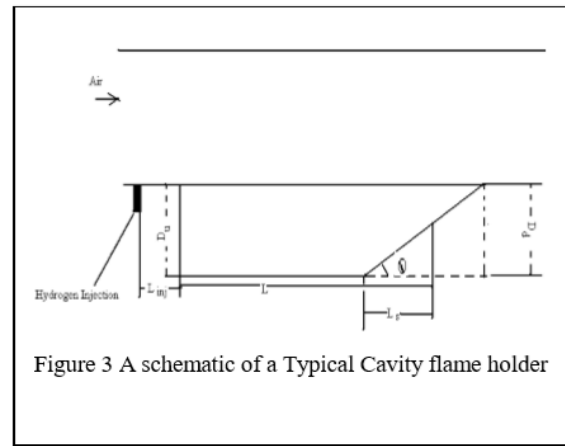


Figure 3 A schematic of a Typical Cavity flame holder

Figure 7 and 8 shows distribution of OH and mass fraction of water vapour. The mixing becomes more predominant in the region far from the jet outlets and heat release gradually increases in the mixing layer between hydrogen and air. The OH mole fraction is less almost by an order to that of water mole fraction. The OH mass fraction decreases as the gas expands around the injected jet and the local mixture temperature falls. However OH species are primarily produced in the hot separation region upstream of the jet exit and behind the bow shock and convected down stream with shear layer. The OH emission of the flame has been imaged for $57 < x < 300$ m and global visualization allows to estimate the mixing and ignition length of hydrogen within the supersonic flow of air. The water mass fraction values at core region could not established exactly. Static pressure distribution along the bottom wall for without cavity has been shown in figure 9 and 10 at different x and y location. The initial pressure rise is

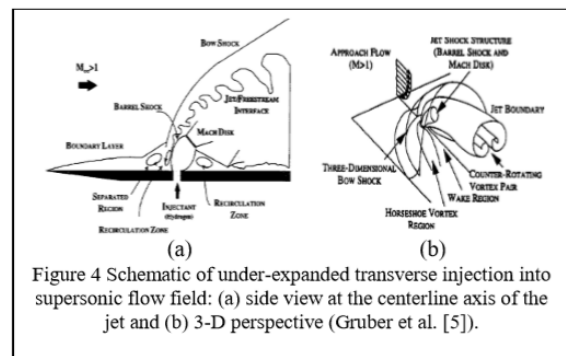


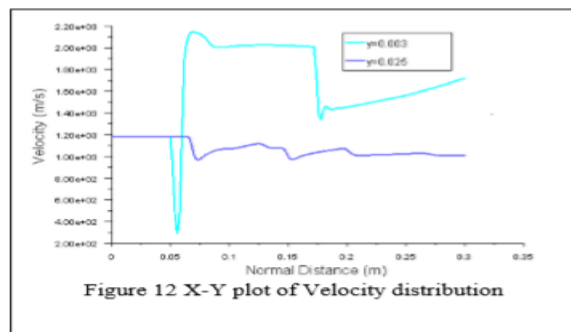
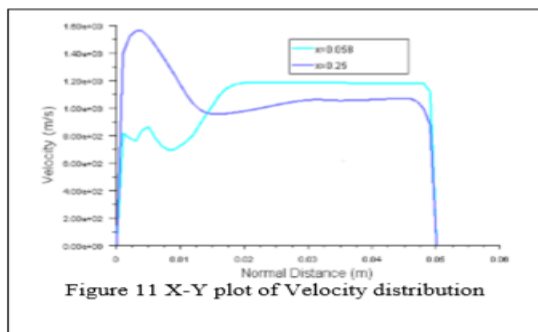
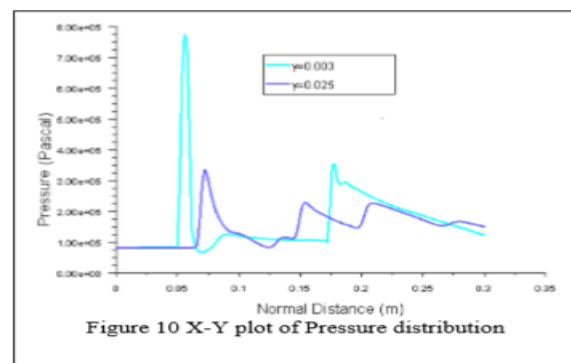
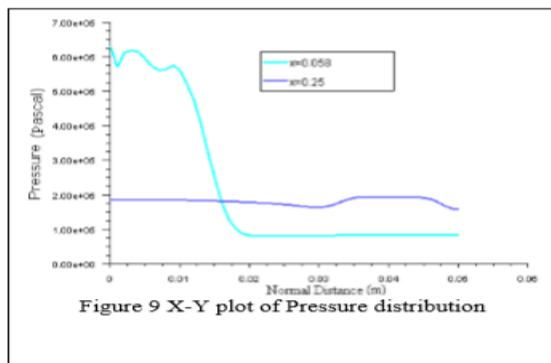
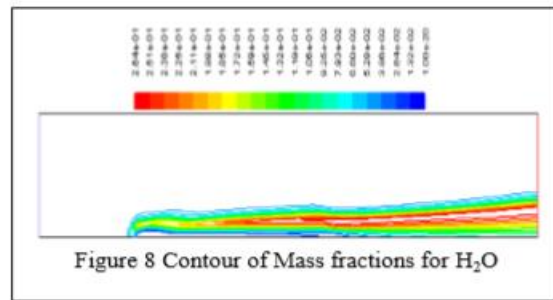
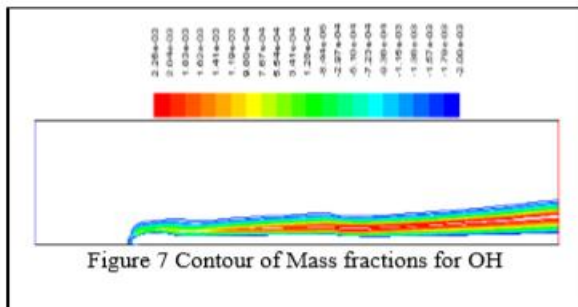
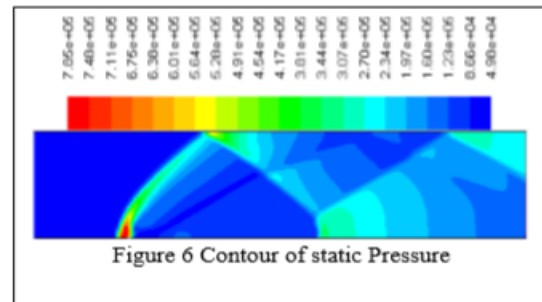
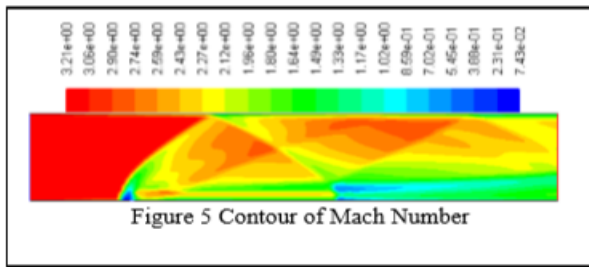
Figure 4 Schematic of under-expanded transverse injection into supersonic flow field: (a) side view at the centerline axis of the jet and (b) 3-D perspective (Gruber et al. [5]).

due to shock wave generated from the downstream region of the injector. There is variation in pressure at $x=0.058$ m near the injector due to expansion fan while at $x=0.25$ m i.e. near the exit of the combustion chamber, is almost constant while near the upper wall there is little variation in pressure due to bow shock. The static pressure is comparatively high at $x=0.058$ m than $x=0.25$ m, this is because of hydrogen is injected at $x=0.057$ m and from the figure 9 it is clearly visualized that there is variation near the lower wall due to recirculation region and barrel shock. The same x-y plot for pressure distribution comes in figure 10 at $y=0.003$ that means near lower wall and $y=0.025$ i.e. in center of the combustion chamber. As it is clear in figure 9 near the injector pressure is high, the same pattern can be seen here



in figure 10. velocity magnitude distribution along the bottom wall for without cavity has been shown in figure 11 and 12 at different x and y location The variation of velocity magnitude along $x=0.25$ is higher compared to the $x=0.25m$ near the lower wall shown in figure 11,

while the velocity magnitude almost constant in the center of combustion chamber. There is lot of variation in velocity magnitude near the injector due to recirculation zone, bow shock and barrel shock in figure 12.



III. CONCLUSION

The current analysis is validated the CFD solver for external supersonic combustion of H₂/air. In the contour of temperature profile within a very short time combustion takes place and reaches up to 27.2e+03 k and near the flame front it can be easily visualize that some form of shock wave is created. The pressure rise due to the combustion is not very high on account of global equivalence ratio being quite low. Within the inlet the shock-wave-boundary- layer interactions play a significant role. Fluctuation in pressure and Mach

number was due to shock train. Without cavity the maximum flame temperature reaches up to 2.74e+03K at $x=0.18m$. This increase in mixing results in an increased entrainment level into the cavity which may lead to a higher level of stability from passive upstream fueling and/or make independent cavity fueling more difficult due to the potential for a richer environment inside the cavity flame holder. In case of without under backpressure the static pressure in the region of the cavity was increased 3.5 times from the nominal levels. Ignition and combustion produced a pre-combustion shock train,

resulting in dual-mode combustor operation. The shock train became stronger and the starting location of the shock train moved progressively upstream with increasing fuel-air equivalence ratio.

ACKNOWLEDGEMENT

The authors acknowledge the financial help provided by AICTE from the project AICTE: 8023/RID/BOIII/NCP(21) 2007-2008 .The Project id at IIT Guwahati is ME/P/USD/4.

REFERENCES

- V.A. Zabaykin and A.A. Smogolev, "3-D Structure Of Hydrogen Flame In Supersonic high-Enthalpy Flow," West-East High Speed Flow Field Conference 19-22, November 2007 Moscow, Russia.
- AntonellaIngenito and Claudio Bruno, "Physics and Regimes of Supersonic Combustion", AIAA Journal, Vol. 48, No. 3, March 2010.
- J. H. Tien, and R. J. Stalker, "Release of Chemical Energy by Combustion in a Supersonic Mixing Layer of Hydrogen and Air", COMBUSTION AND FLAME 130:329-348 (2002).
- Adela Ben-Yakar and Ronald K. Hanson, "Cavity Flame-Holders for Ignition and Flame Stabilization in Scramjets: An Overview", Journal Of Propulsion And Power Vol. 17, No. 4, July-August 2001.
- Jeong-Yeol Choi, Fuhua Ma and Vigor Yang, " Dynamics Combustion Characteristics in Scramjet Combustors with Transverse Fuel Injection", 41st AIAA/ASME/SAE/ASEE Joint Propulsion Conference & Exhibit 10 - 13 July 2005, Tucson, Arizona, AIAA 2005-4428.
- T. K. G. Anavaradham, B. U. Chandra, V. Babu and S. R. Chakravarthy and S. Panneerselvam Experimental and numerical investigation of confined unsteady supersonic flow over cavities", The Aeronautical Journal March 2004 pp.135-144.
- A. Ben-Yakar and R. K. Hanson, "Experimental Investigation Of Flame-Holding Capability of Hydrogen Transverse Jet In Supersonic Cross-Flow", Twenty-Seventh Symposium (International) on Combustion/The Combustion Institute, 1998/pp. 2173-2180.
- Tianwen Fang, Meng Ding, Jin Zhou, "Supersonic Flows Over Cavities", Front. Energy Power Engineering. China 2008, 2(4): 528-533
- In-Seuck Jeung and Jeong-Yeol Choi, "Numerical Simulation of Supersonic Combustion for Hypersonic Propulsion", 5th Asia-Pacific Conference on Combustion,The University of Adelaide, Adelaide, Australia 18-20 July 2005.
- Kyung Moo Kim, Seung Wook Baek and Cho Young Han Numerical study on supersonic combustion with cavity-based fuel injection", International Journal of Heat and Mass Transfer 47 (2004) 271-286.
- Tarun Mathur, "Supersonic Combustion Experiments with a Cavity-Based Fuel Injector", Journal of Propulsion and Power Vol. 17, No. 6, November-December 2001.
- J. Philip Drummond, Glenn S. Diskin, and Andrew D. Cutler, "Fuel-Air Mixing And Combustion In Scramjets", American Institute of Astronautics and Aeronautics (AIAA-.2002-3878).
- Yves Burtschell, GhislainTchuenb and David E. Zeitoun, "H2 injection and combustion in a Mach 5 air inlet through a ViscousMach Interaction", European Journal of Mechanics B/Fluids 29 (2010) pp.351-356.
- D. Haworth, B. Cuenot, T. Poinot, and R. Blint, "Numerical simulation of turbulentpropane-air combustion with non-homogeneous reactants: initial results", Center for Turbulence Research Proceedings of the Summer Program 1998, pp.5-24.
- YiguangJu and Takashi Niioka, "Ignition Simulation of Methane/Hydrogen Mixtures in a Supersonic Mixing Layer", Combustionand Flame 102:462-470 (1995)
- Nitin K. Gupta, Basant K. Gupta, Narayan Ananthkrishnan_Gopal R. Shevare,IkSoo Park and Hyun Gull Yoon, "Integrated Modeling and Simulation of an Air-breathing Combustion System Dynamics", American Institute of Aeronautics and Astronautics, pp.1-31.
- M. Akbarzadeh and M. J. Kermani, "Numerical Computation of Supersonic-Subsonic Ramjet Inlets; a Design Procedure", 15th. Annual (International) Conference on Mechanical Engineering-ISME2007 May 15-17, 2007, Amirkabir University of Technology, Tehran, Iran ISME2007-3056.
- Stephen J. Mattick and Steven H. Frankel, "Numerical Modeling of Supersonic Combustion:Validation and Vitation Studies Using FLUENT", 41st AIAA/ASME/SAE/ASEE Joint Propulsion Conference & Exhibit, 10 - 13 July 2005, Tucson, Arizona, AIAA 2005-4287
- A. Balabel, A.M. Hegab, S. Wilson, M. Nasr, S. El-Behery, "Numerical Simulation of Turbulent Gas Flow in a Solid Rocket Motor Nozzle", 13th International Conference on Aerospace Sciences & Aviation Technology, ASAT- 13, May 26 - 28, 2009, Paper: ASAT-13-pp-13.
- A.T. Sriram and D. Chakroborty "Numerical Simulations Of Staged Transverse Injection Into Mach 2 Flow Behind Backward-Facing Step", Proceedings of the International Conference on Aerospace Science and Technology,26 - 28 June 2008, Bangalore, India, INCAST 2008-119.

AUTHOR PROFILE



Dr. K.M. Pandey did his PhD in Mechanical Engineering in 1994 from IIT Kanpur. He has published and presented 170 papers in International & National Conferences and Journals. Currently he is working as Professor of the Mechanical .Engineering Department, National Institute of Technology, Silchar, Assam, India. He also served the department in the capacity of head from July 07 to 13 July 2010.

He has also worked as faculty consultant in Colombo Plan Staff College, Manila, Philippines as seconded faculty from Government of India. His research interest areas are the following: Combustion, High Speed Flows, Technical Education, Fuzzy Logic and Neural Nnetworks ,



Heat Transfer, Internal Combustion Engines, Human Resource Management,
Gas Dynamics and Numerical Simulations in CFD area from
Commercial Softwares. Email:kmpandey2001@yahoo.com.



Mr. AdityaPratap Singh did his M-Tech in Thermal Engineering in 2008 from NIT Silchar. He has published and presented Many papers in International & National Conferences and Journals. Currently he has submitted his PhD thesis in Department of Mechanical Engineering, National Institute of Technology, Silchar, Assam, India.. His research interest areas are the following; Gas Dynamics, Combustion, High Speed Flows, Numerical Methods in Fluid Flow and Heat Transfer. Email:hello2apsingh@gmail.com.